THE INFLUENCE OF WATER ON THE DEGRADATION AND WEAR OF AL2O3

SURFACES

A Thesis

by

AMMON TERRY PICKETT

Submitted to the Office of Graduate Studies of
Texas A&M University
in partial fulfillment of the requirements for the degree of

MASTER OF SCIENCE

August 2008

Major Subject: Chemistry

THE INFLUENCE OF WATER ON THE DEGRADATION AND WEAR OF AL2O3

SURFACES

A Thesis

by

AMMON TERRY PICKETT

Submitted to the Office of Graduate Studies of
Texas A&M University
in partial fulfillment of the requirements for the degree of

MASTER OF SCIENCE

Approved by:

Chair of Committee,	James D. Batteas
Committee Members,	Paul S. Cremer
	Daniel F. Shantz
	Dong Hee Son
Head of Department,	David Russell

August 2008

Major Subject: Chemistry

ABSTRACT

The Influence of Water on the Degradation and Wear of Al_2O_3 Surfaces.

(August 2008)

Ammon Terry Pickett, B.S., Southern Utah University

Chair of Advisory Committee: Dr. James D. Batteas

As alumina plays ever more important roles in advanced technologies, such as substrates for in vivo biological sensors, catalysts for water purification and components of novel fuel devices, it is exposed to various environments. These environments lead to wear and degradation due to chemical and mechanical forces. Macroscale tribological tests including the scratch test and indentation are unable to analyze nanoscale properties due to their limited sensitivity. Today, nanotribologists incorporate three main tools to analyze nanoscale tribological properties: atomic force microscopy (AFM), the nanoindentor and surface force apparatus. Of these, AFM is the instrument of choice due to the sensitivity to and diversity of surface properties analyzed in a single setting. Through adhesion measurements and scratch testing under known loads the AFM was used to analyze the effect of OH^- on the degradation of the alumina surface. Fourier transform infrared spectroscopy (FTIR) and AFM were also used to analyze the stability of self-assembled monolayers (SAMs) on the alumina surface.

Through scanning a region of the surface with a defined force in an aqueous environment, the tribochemical surface properties were found. The pressure required to

induce degradation of the first O-Al layer (~2 Å) ranged from 3.10 GPa at a pH 3 to 1.58 GPa at pH 10. Further analysis of adhesion across the surface and within a defect region exposed significant changes in the forces of adhesion as the alumina surface experienced wear. At pH 3, 5, 7, and 10 the adhesion was approximately double that of the defect free surface.

Two well known molecules were examined for their ability to protect the surface from bond rupture due to the catalytic effect of OH$^-$. SAMs of octadyclephosphonic acid (OPA) and Octadycletrichlorosilane (OTS) were assembled on the alumina surface. FTIR spectra indicated well ordered monolayers formed from each molecule. The exposure of OPA to aqueous environments of pH >7 lead to the degradation of the SAM. OTS, on the other hand, demonstrated significantly more resilience to degradation as indicated through FTIR and AFM analysis.

DEDICATION

I dedicate this thesis to my family. To a wonderful wife who has supported me in this great endeavor. To my children, who have lightened my mind with regular reviews of Dr. Seuss and other light reading.

ACKNOWLEDGEMENTS

NOMENCLATURE

AFM	Atomic Force Microscopy
OTS	Octadecyltrimethoxy Silane
OPA	Octadecyl Phosphonic Acid
SAM	Self-Assembled Monolayer
FT-IR	Fourier Transform Infrared
THF	Tetrahydrofuran
IEP	Isoelectric Point
STM	Scanning Tunneling Microscopy

TABLE OF CONTENTS

LIST OF FIGURES

1. INTRODUCTION

As advancing technologies push towards the micro and nanoscale regime the effect of atomic wear becomes more apparent as the ratio of defect size and surface area increases. This becomes more important as their effects cause more noticeable degradation in micro and nanosystems. In the past, wear on the nanoscale has been largely overlooked in macrosystems due to lack of instruments able to analyze them. But now, as researchers look more into nanomaterials, it has been found that as the ratio of surface area to bulk area increases, the effect of defect nucleation becomes more severe.[1] Thus, the importance of understanding defect nucleation and methods to prevent it have become great.

Alumina (Al_2O_3) is a material found to be very useful in areas such as biotechnology, fuel cells, water treatment, and micro/nanoelectromechanical systems (MEMS/NEMS). In a recent study on the biocompatibility of different brain implants, single crystal alumina was placed in the brain of a rat for up to 90 days and then analyzed for changes in topography.[2] Alumina was found to be more robust than silicon when exposed to the rat's brain, though it was still subject to some degree of degradation. As one can imagine if a sensing device were to be placed in one's brain, any corrosion/wear caused by the environment would be detrimental.

Energy concerns have grown considerably in the past years and many researchers are seeking alternative, clean energy sources. Alumina has found application in some of

_____

This thesis follows the style of *Langmuir*.

the new energy technologies, such as that of solid oxide fuel cells (SOFC). A SOFC is a device that uses electrochemistry to created electricity. They consist of an anode and cathode separated by a conducting material. Fuel such as O_2, H_2O steam and CO_2 are reacted on the electrodes and current is formed by the electron flow. In one study, alumina was found to increase both the mechanical and electrical potential of SOFC. When alumina was co-precipitated with ZrO_2, a common electrolyte material, the fuel cell showed greater bending strength which leads to a more robust material. Also, the addition of alumina improved the resistivity and impedance of the cell, while the conductivity was slightly decreased.[3]

Alumina has been found to be a useful catalyst for treating water with current methods, such as ozonation[4, 5] and irradiation[6]. A common problem is that some organic molecules are very robust to regular treatment procedures, such as 2-chlorophenol. In one study on the degradation of 2-chlorophenol, alumina was found to improve the ozonation of 2-chlorophenol by 83.7% in an acidic environment and at the same time reduce the amount of ozone required by 39.5%.[5] Alumina attracts 2-chlorophenol to the surface where it is decomposed with ozone and radical ·OH molecules that were produced from the alumina.

Thus alumina has become a material of high interest in up-coming technologies, and the importance in understanding the process of wear and degradation in different environments has become ever more apparent. Due to the various environments in which it is exposed (i.e. brain implants), it is important to understand how the

environment may affect the stability of the material, how it may lead to wear or degradation and how it may be avoided in order to improve its lifetime.

To begin a study of alumina, the structure and its relevance to wear and degradation must be known. Alumina is found in a variety of transition structures that are usually dictated by the presence of hydroxide in the crystal matrix and by the temperature at crystal formation. The alumina of interest in this research is α-alumina, which is the crystal structure that corresponds to corundum. The results of this research should be applicable to the other transition species that are also commonly found, due to the hydroxylation of the surface in aqueous environments.[7] The crystal plane that was investigated in this research was the (0001) basal plane. The crystal structure in this plane consists of layers of oxygen in a hexagonal closed pack arrangement sandwiching a layer of aluminum atoms dispersed close to the oxygen layer above or below.

Alumina is an amphoteric material in which the aqueous environment greatly affects the surface charge, creating a positive or negative charge across the surface. The point at which there are no charges on the surface is the isoelectric point (IEP), or point of zero charge. For alumina this has been a subject of much debate due to varied findings.[4, 8-13] The errors reported are attributed to either the presence of silica particles at the surface or a roughened surface caused by plasma cleaning.[4] Recently, with more accurate measurements, the consensus is that the IEP for single crystal alumina (0001) is around pH 6.[8, 13, 14]

The amphoteric nature of alumina affects much of the chemistry on the alumina surface. Water is known to create charges across alumina as water molecules interact

with the surface.[7, 15] Positive and negative charges are created as the pH falls below or rises above the IEP. When the pH is below the IEP the surface will be dominated by $AlOH_2^+$ molecules, at the IEP by $AlOH$, and above the IEP by AlO^-. Many of the known molecules that bind to alumina rely on the surface charge for binding events to take place. For example[16], carboxylic acids form various complexes on the alumina surface. The most stable method of attachment has been found to occur when the pH is around 3-4 and is improved in this range because the carboxylic acid has been deprotonated, giving it a negative charge, and the alumina surface remains positively charged, due to the pH below the IEP.   This coulombic attraction causes migration of the carboxylic acid to the surface where it is chemically bound.

Other studies have investigated silane[17-19] and phosphonic acid[20-27] attachment at the surface which is a little more complicated due to the competitive binding of water. The key to attachment of silane and phosphonic acid molecules to the alumina surface is to have a water free environment. *Psuedonomas* are a type of bacteria that are found to corrode alumina and steel. *Psuedonomas* contain species that are present in fuel, ocean water and other liquids that are commonly exposed to alumina. In one study, OTS SAMS were formed on alumina in an effort to reduce the corrosion caused by microbes. A SAM of OTS was formed using toluene as the solvent. The application of a SAM of OTS decreased the corrosion rate by 61%.[19]

In a theoretical study on the binding of phosphonic acid molecules, it was found through density functional theory calculations that the binding between the alumina surface and the phosphonic head group happens more readily through a condensation

reaction. The condensation reaction leads to a tridentate bond to the alumina surface.[27] Theoretically this should lead to a more stable monolayer on the surface and was supported by Foster in a comparative study on SAMs of thiols on gold and phosphonic acids on alumina. It was found that in ambient conditions phosphonic acid SAMs would retained their coefficient of friction after 700 hrs compared to SAMs of thiols that decreased in a approximately 24 hrs.[28] The decrease in the coefficient of friction relates to the breakdown of the SAM due to oxidation.

The study of wear, adhesion, lubrication and other related surface properties falls under the encompassing study of tribology. In the past, tribologists have incorporated such techniques as indentation[1, 29-31] and scratch tests[32-34] to evaluate the macroscale hardness, friction and wear of materials. To examine the relative stability of different crystallographic planes to abrasion, alumina samples were worn with boron carbide abrasives. From these studies, it was found that the (1011) was more prone to abrasion than the (0001) plane with a difference in 34 J/m^2.[33] In typical indentation tests, a pyramid shaped indenter is forced into a material. Tribologists are interested in the amount of force required to penetrate the surface and the types of defects formed from the indentation. There has been an apparent deviation from the ideal shear strength of materials from the results found in macroscale experiments. As the tribological techniques evolve to achieve smaller scale sampling, researchers have obtained much closer shear strength results. For example, Minor *et al* observed a shear strength of 1.95 GPa, which is very close to the theoretical value of 2.2 GPa, in a nanoindentation experiment on aluminum.[29]

More recently tribological research has been taken to the nanoscale with the use of atomic force microscopy (AFM).[35-46] In one study, on the wear of calcite, atomic layers of wear were observed under an aqueous environment. They found that wear was limited by the chemical reaction of the surface and independent of the scanning done by the AFM tip.[44] With the scanning of the tip, however, the wear of step edges was imaged, and the process of degradation was mapped. This is an example of the insights AFM has brought to tribological studies.

In materials such as alumina, multiple factors come into play in the process of wear. There is a mechanical component caused by direct contact with other surfaces, and there is a chemical component that catalyzes the wear of ceramics. It has been found that these two components work hand-in-hand, and when singled out neither mechanical nor chemical influences affect defect formation to a significant degree.[15]

Defect nucleation is where forces on the surface, both chemical and mechanical, cause bond breakage, which in time will lead to gross wear.[15, 31, 32] Though it is known that this event occurs, actual monitoring of defect nucleation has been difficult. The difficulty arises from lack of atomically sensitive analytical tools and from little need to understand this process due to the relatively minor effect that it has on mechanical components in the macroscale. Today, however, there is a need and a way to analyze defect nucleation. In a recent study[41] on mica, AFM was used to monitor defect nucleation at the nanoscale under aqueous conditions. At pH 3, 5 and 8, the OH^- concentration at the surface could be controlled in such a way that the effect of strain on bond breaking could be separated from the chemically induced bond breaking catalyzed

by OH⁻ ions. This method may also be applied to the analysis of defect nucleation on the alumina surface.

For nanotribologists, AFM is an ideal candidate for the interrogation of physical processes that take place in the nanoscale.[37, 41, 47-50] The AFM uses an extremely sensitive cantilever system to monitor and assess atomic forces present when two bodies are brought into contact. At the end of the cantilever is a very small tip used to probe the forces of the surface of interest. A laser is positioned above the tip on the cantilever and then deflected onto the center of a quadrant detector. As the tip is raster scanned across a defined area of the surface the forces acting on the tip will cause shifts in the deflection of the laser to the sensor. A feedback loop regulates the force applied to the cantilever as changes in forces between the surface and tip are monitored. The forces are translated into forces of friction and topography changes, which allow for simultaneous data collection of friction variations on the surface as well as topographical changes.

Besides friction and topography data, an AFM is also a very sensitive device for analyzing adhesion forces between the surface and tip. Due to the small radius of curvature of the tip, atomic scale forces of adhesion can be probed. Figure 1 depicts the adhesion measurements as a tip is brought into and out of contact with a surface. As the tip is retracted from the surface the adhesive force holds the tip to the surface until the force from the AFM overcomes the adhesion, and the tip snaps away from the surface.

Figure 1. Force Distance Diagram. Depiction of tip movement in a force/distance plot following actual approach (blue line) and retract (red line) on alumina.
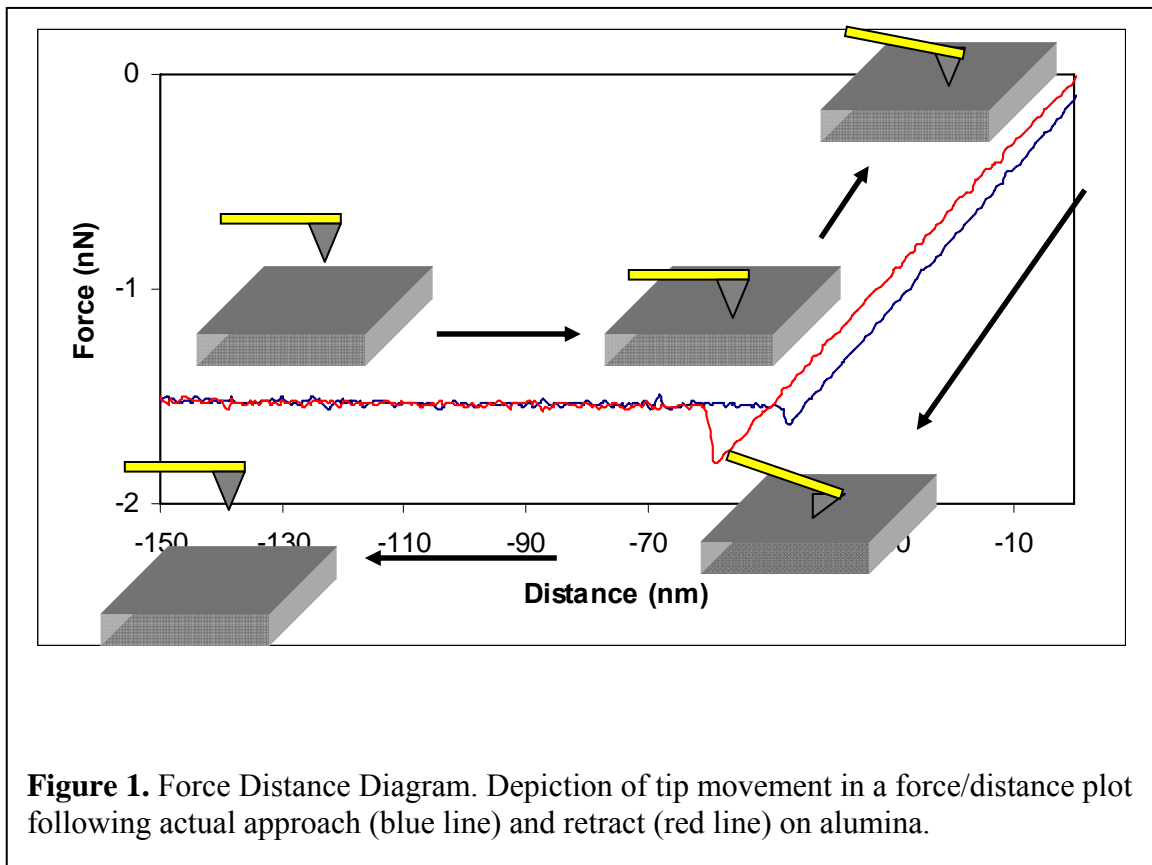
The difference between the forces exerted to release the tip and the normal force exerted by the AFM when the tip is away from the surface is the amount of adhesion force caused from the two-body interaction. Hertz first described the fundamentals of contact in the event of two curved surfaces contacting each other. The model Hertz used was one of none deforming, two body contact in an elastic collision.[51] Two prominent additions to the Hertz model came from Johnson, Kendall and Roberts (JKR)[52] and from Derjaguin, Muller and Toporov (DMT).[53] In these two models, interfacial attraction of

soft material contact (JKR) and hard solid contact (DMT) were included in the derivation of adhesion resulting from the collision.

In order to increase understanding of the data collected, the AFM tip can be chemically modified so that as adhesion measurements are taken, chemically significant forces can be assumed. This is done in a number of ways, the simplest of which is to oxidize the surface of the tip. For example, a silicon nitride tip can be oxidized using an RCA cleaning solution (4:1:1 H_2O, H_2O_2 and NH_4OH respectively) to produce a tip with a silanol terminated silica layer which is chemically clean and stable.[41]

The AFM is a versatile instrument which can be used in a number of different environments depending on the needs of the investigation. Experiments have been conducted in air, in many different types of liquids, in vacuum, with specialized tips coated with different molecules, with adjustable temperature and with applied current through conductive tips. Basic AFM can be conducted on most any surface within reasonable surface roughness, which distinguishes it from scanning tunneling microscopy (STM) which requires a conductive substrate.

While the AFM can provide surface structural data, it does not normally provide chemically specific information in the way that spectroscopy does. Thus, when characterizing surfaces, chemical information from spectroscopic tools is also of importance. To obtain molecular information, Fourier transform infrared spectroscopy (FTIR) is used in this study. FTIR spectroscopy was used in transmission mode for this investigation due to the transparency of double side polished alumina substrate. For the alkyl chains, FTIR spectroscopy analyzed the methylene symmetric and asymmetric

stretching vibrations. The peaks relating to methylene have been found to shift according to the organization of the monolayer on a surface. The methylene asymmetric peak, associated with well ordered self-assembled monolayers, arises at ca. 2918 cm^{-1} and will shift to higher frequencies as the film becomes less ordered.[54] Thus the extent of order within the film can be derived from IR spectroscopy.

This investigation explores how aqueous conditions affect the wear of single crystal Al_2O_3 (0001) and the binding of two potential surface protecting groups. The objective of this study is to shed light to the effect of environment on corrosion and wear, so that the future use of alumina, for applications such as implants, will be safe and more effectively used. Also, that a general model for the corrosion and wear of any aluminum oxides might be drawn from the data and results obtained through this research endeavor.

2. DEGRADATION AND WEAR OF BARE ALUMINA (0001)

2.1 Overview

The degradation of alumina decreases the lifetime and reliability of modern devices. Wear and corrosion are the main causes of alumina degradation and in many instances work together to increase the rate of degradation due to the chemical (corrosion) and mechanical (wear) environments in which it is commonly exposed. In order to resolve the effects of environment, defect nucleation on alumina was investigated through a series of experiments at various pH using AFM. AFM was selected due to its sensitivity to atomic forces and image resolution down to 0.1 nm which make it ideal for observing the process of defect nucleation.

In this study, the corrosion process of concern was the water based reaction with the alumina surface. The reaction was controlled through regulation of the pH, allowing more H^+ or OH^- to attack the surface. The pH was changed using HCl or NH_4OH to decrease or increase the pH and was monitored by a pH meter to obtain specified pH.

Mechanical wear was introduced through the application of specific loads on to the AFM as it is raster scanned across a defined area of the surface. The force exerted by the AFM during a series of loaded scans was calculated using the Hertz mean pressure calculation which has been outlined elsewhere.[41, 55, 56] After a defect is formed, surfaces typically go through structural shifts to attain a lower energy state. The defect, in this case, is the result of broken bonds, thus creating energy variation on the surface that needs to be passivated in order to reach a more stable energy state. Force distance

spectroscopy was used to measure adhesion as the AFM tip is brought into and out of contact with the surface. The adhesion of two contacting bodies

2.2 Experimental

The sample preparation method was as follows: polished single crystal alumina (0001) substrates (Crystal Systems, Inc) were cleaned of all carbon contaminants. This cleaning process included 20 min UV/ozone cleaning and 20 min in a 4:1:1 solution of H_2O, H_2O_2 and NH_4OH. The substrate was then rinsed with ultrapure water (18 $M\Omega*cm$) and blown dry with nitrogen gas.

The AFM tips were cleaned and oxidized in a 4:1:1 solution of $H_2O/H_2O_2/NH_4OH$ for ~5min.[35] This cleaning oxidized the tip, creating a layer of SiO_2 over the silicon nitride, and thus allows chemical and physical surface properties to be derived through the IEP of alumina (~pH 6) and silica (pH ~3.5) in different pH environments. The tip shape was calibrated through a previously described method[57] by scanning it over a $SrTiO_3$ (305) surface with sharp well defined features. This allows a mapping of the tip size as the edges of the $SrTiO_3$ are much sharper than the tip.[50]

Investigation of bond cleavage was analyzed using the AFM (Molecular Imaging PicoSPM connected to an RHK Technology SPM 1000 Electronics). The AFM works through the detection of tip height and twisting caused by the interaction of the tip with the surface being studied. A laser is directed to the cantilever directly above the tip and the laser is then deflected to a quadrant detector. A feedback loop monitors the changes in the deflection of the laser on the detector as the tip is scanned across a surface, height

variations are detected and adjustments are made to maintain contact with the surface. Pressure, or load, is applied to the tip through changing the electricity applied to the piezoelectric core. The voltage applied to the piezoelectric core causes the material to expand or contract. Thus when voltage is applied to the piezoelectric 'z' core the AFM tip is pushed towards the surface, increasing the pressure of the tip against the surface.
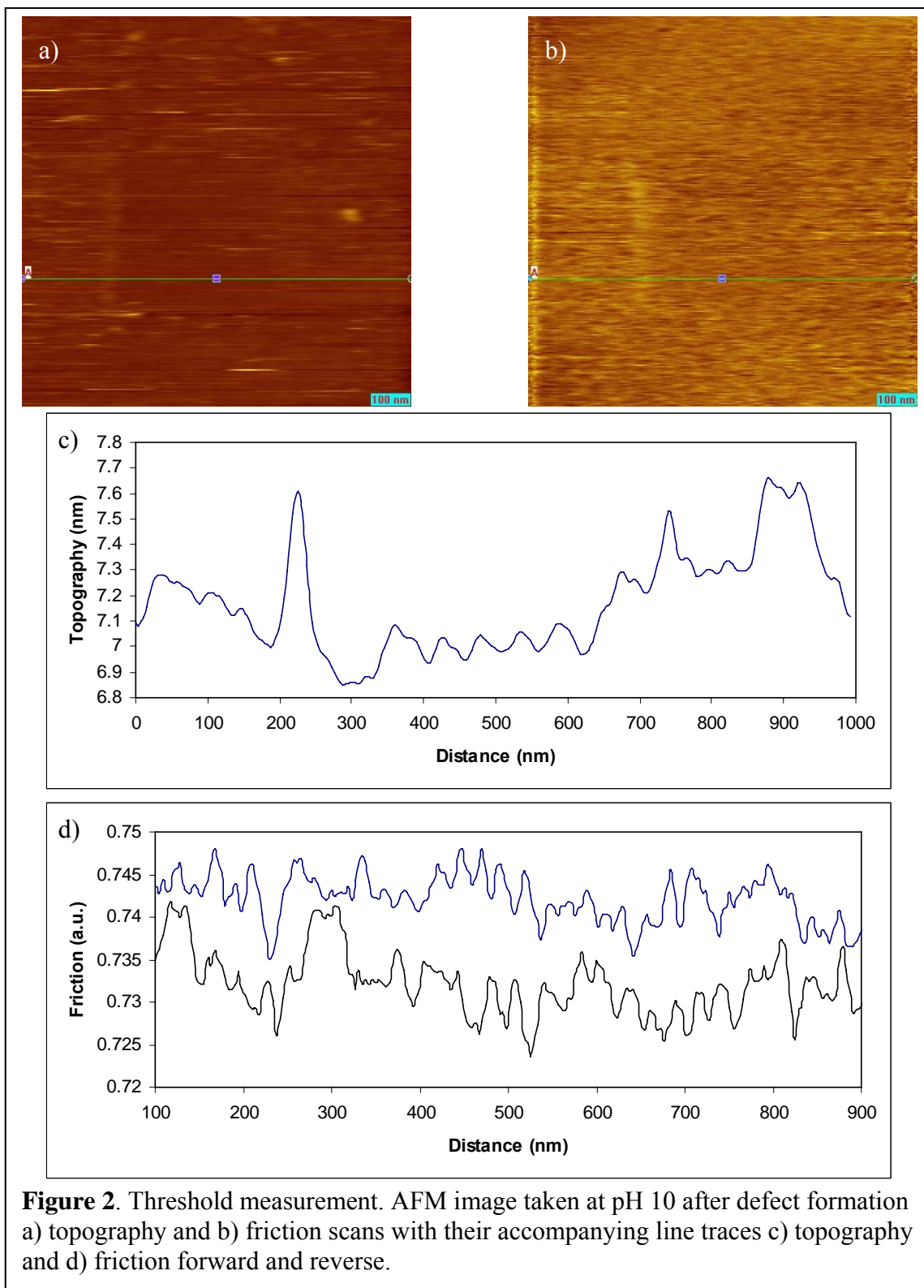
The approach to be taken to investigate the wear of alumina (0001) at the nano-scale rests on the AFM analysis of polished alumina (0001) under different aqueous environments. The aqueous environments will be at pH 3, 7 and 10 so that the gamut of environments exposed may be analyzed around the IEP. The AFM tip will probe the chemical/mechanical wear occasioned by the scanning of the surface at the minimum load (threshold pressure) required to cause approximately 2 Å (first O-Al layer) of wear in 10 scans at 33 Hz. Under controlled high loads, the tip scans a 400×400 nm^2 area, and at lower loads, the tip will observe the damage inflicted by the higher loaded scans by scanning a larger area (1×1 μm^2). In this study, loads ranged from 1.65 nN to 12.5 nN.
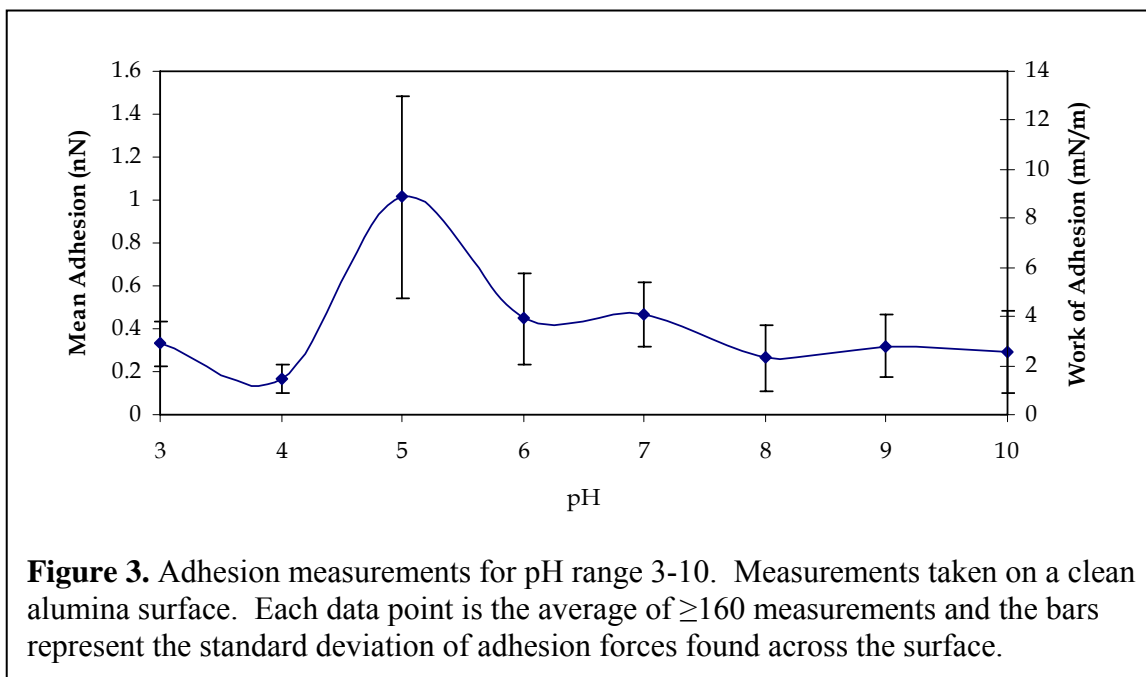
Investigations of adhesion were made through force distance spectroscopy. The point when the tip leaves the surface there is a snapping of the tip away from the surface which results in a vertical shift in the graphical representation, Figure 1. A measure of the vertical height can lead to a measurement of the amount of attraction or adhesion the surface has toward the AFM tip.

2.3 Results

Wear threshold analysis on alumina brought to light the pH dependence of bond breaking leading to wear. It was found that as the pH of the environment increased, the force required to induce defects decreased. The line trace of Figure 2a shows a depth of ~2 Å, though there is build up along the edges of the defect scan area leading to large peaks spaced ~400 nm apart. Forward and reverse friction images were shown in Figure 2d. Typically from comparing the frictional differences in wear areas, one can monitor changes in friction from the native surface to the defect region. In the measurements found during this study, very little frictional change was measured.

Though there was little frictional change found, there was a substantial change found in the threshold pressure as the pH was changed. More specifically, at a pH of 3 the threshold pressure was found to be 3.10 GPa and decreased to 1.58 GPa at a pH of 10. This ~1.5 GPa decrease can be attributed to the increased concentration of hydroxide molecules on the surface. It is known that OH⁻ catalyzes the breaking of M-O-M bonds. In this case, the energy required to break the Al-O bond is decreased as OH⁻ interacts with the surface. This process has also been studied on mica where a similar dependence on hydroxide concentration greatly influenced the ease of causing gross wear. The change in threshold pressure was approximately 1 GPa when the pH was changed from 3 to 8.[41] In the case of mica the OH⁻ interacted with either a Si-O or Al-O bond, which in both cases catalyzes the rupture of bonds as pressure is applied through the AFM tip.

Figure 2. Threshold measurement. AFM image taken at pH 10 after defect formation a) topography and b) friction scans with their accompanying line traces c) topography and d) friction forward and reverse.

Figure 3. Adhesion measurements for pH range 3-10. Measurements taken on a clean alumina surface. Each data point is the average of ≥160 measurements and the bars represent the standard deviation of adhesion forces found across the surface.

When comparing the force of adhesion on bare alumina to the pH of the environment there is a curious trend. Figure 3 shows the forces of adhesion as a function of pH. Each point represents ≥160 adhesion measurements and the bars are the standard deviation of adhesion forces found across the surface. The measurements were taken by moving the tip to a different location after each measurement. Throughout most of the studies, there appears to be little change in the adhesion of the AFM tip to the alumina surface being between 0.2 nN and 0.6 nN. This is likely due to the limited contact radius resulting from the high elastic modulus of silicon nitride and alumina, 220 GPa and 475 GPa respectively.

It is known that silica has an isoelectric point of approximately pH 3, and the isoelectric point of alumina is probably between pH 5 and 6. This may lead to the greater adhesion found at pH 5 as the alumina remains positively charged whereas the silica AFM tip is negatively charged, creating stronger pull caused by coulombic attraction. In a study done comparing the adhesion of an aluminum oxide surface to that of a phosphonic coated surface, it was found that the aluminum oxide surface had an adhesion of ~30 nN. The adhesion was taken in ambient conditions with a silicon nitride tip.[20] There is a major difference in their adhesion results and the results obtained in this study of 1nN on the defect free alumina surface. This is probably due to the interaction of the AFM tip with the water meniscus that is formed in ambient conditions at the tip-surface interface and the possibility of contaminants on the surface. Also, the tip may have been larger which was not mentioned, nor apparently taken into account in the adhesion measurements. In a similar study on mica in aqueous environments, a maximum adhesion was found to be ~10 nN at pH 6.[41] The trend in their reported adhesion vs. pH followed a similar trend as was shown in this research, but in the case of alumina the maximum adhesion was found to be around pH 5.

The greatest difference in adhesion came from the comparison of the adhesion of the polished surface to the adhesion in a tip induced defect area. Adhesion measurements were taken within the defect area to analyze their potential effect on wear. Figure 4 illustrates the differences in adhesion measured in (red) and out (blue) of a defect area. Surprisingly the force of adhesion increased at each pH by approximately double that of the defect free surface. In order to detect if the increased adhesion was a

result of the blunting of the tip, adhesion measurements were taken before the loaded

scans, then in the defect region and then outside of the defect region. The results are

shown in Figure 5, here we see that indeed the adhesion increases in the defect region

and then decreases once adhesion measurements are taken out of the defect area. This

decrease implies that there is negligible wear done on the tip as defect regions are

created. This is also supported by work done by Maw et al[50] where after 25 scans in

Figure 4. Comparison of adhesions measured in (red) and out (out) of the defect region. Values represent the mean of ≥ 80 measurements taken in (red) and out (blue) of a defect area.
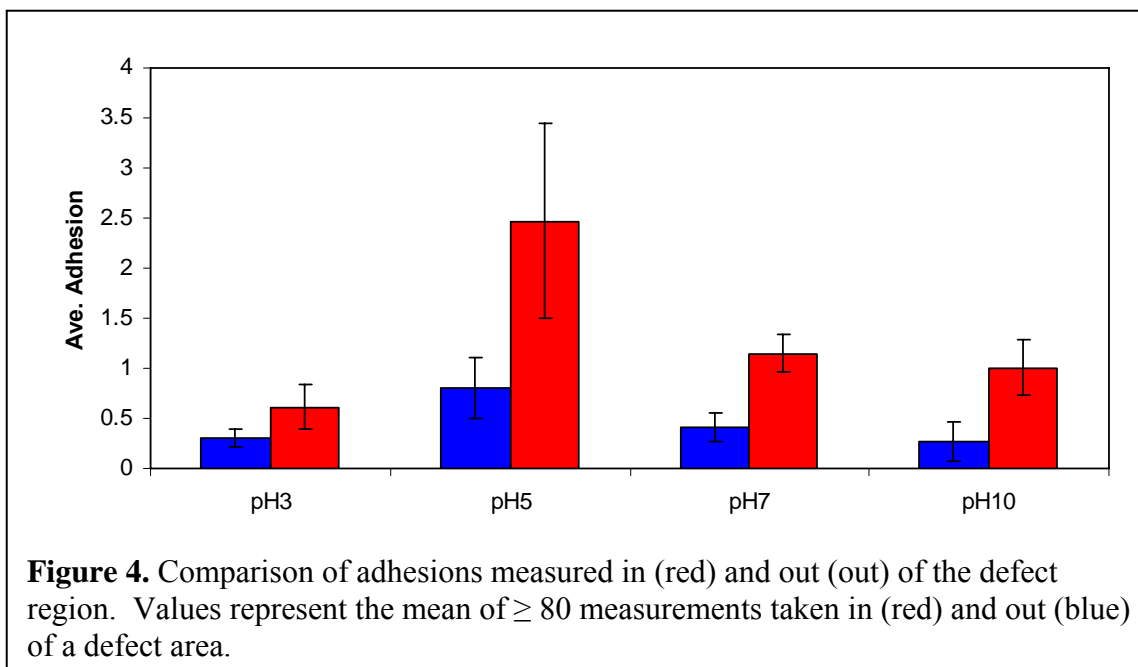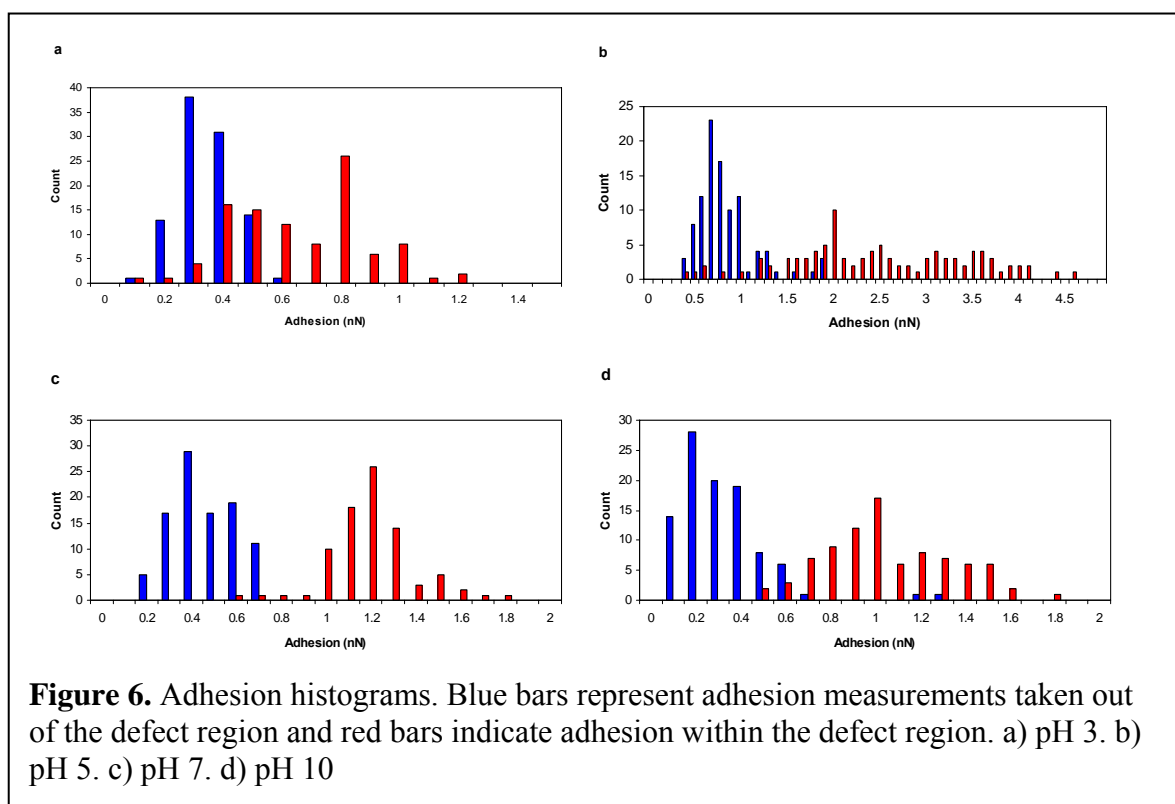
distilled water at a force of 120 nN less than 5 nm of wear was found on the tip. In this

research no more than 12.5 nN was ever applied to the tip so it is unlikely that any

significant wear took place on the tip. Figure 6 gives a more in-depth look at the spread of adhesion at various environments in and out of defect regions. Figure 6 shows the histogram for each individual trial, which further substantiates the distinct adhesive difference between the alumina surface and a defect region as there is little overlap in the measurements taken.

Figure 5. Comparison of tip adhesion before and after defect nucleation. Measurements taken at pH of 5 and figures represent the mean of ~50 measurements. Bars represent the first standard deviation of adhesion measured within an area of the surface.
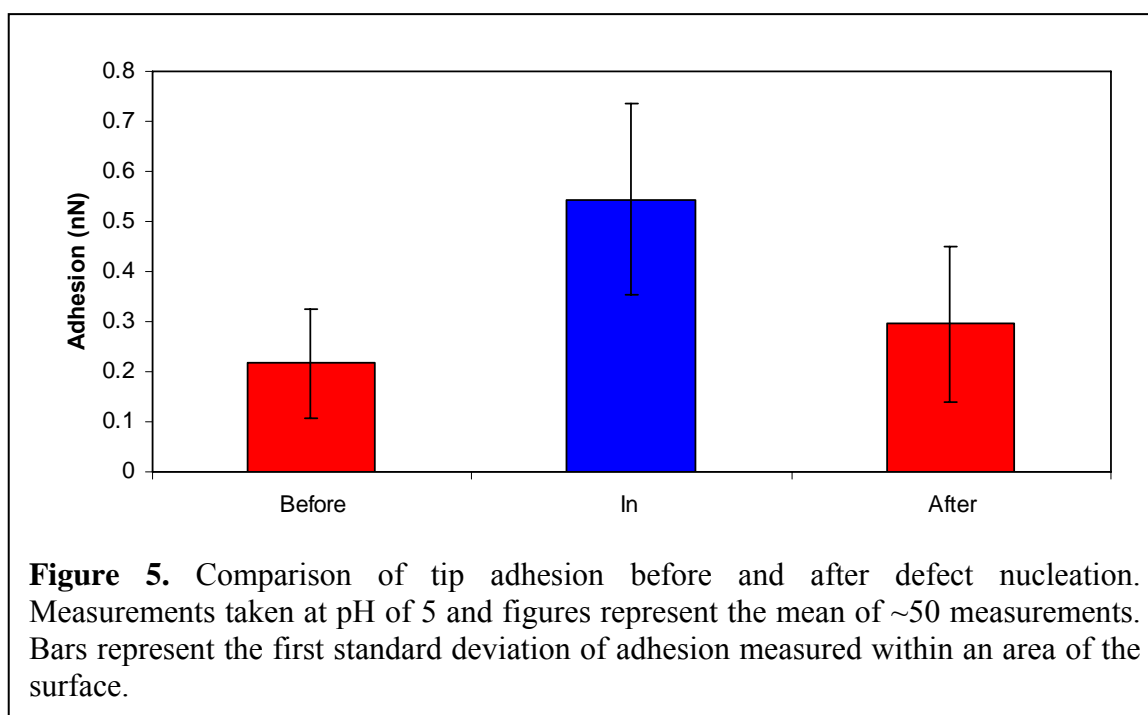
In evaluating the causes that might lead to the increase in adhesion, the fundamental cause must be a result of increased interfacial forces. Interfacial forces may result from greater contact area and/or changes in the surface chemistry. As mentioned

previously, 120 nN of applied force on a silicon nitride tip being scanned across an alumina surface caused an insignificant amount of wear on the tip. Since the radius of the tip is not increasing significantly, then an increase in contact area would likely be due to greater tip penetration. A local decrease in the Young's modulus would allow the AFM tip to penetrate the surface more, which could lead to increased adhesion. In metals such as iron and aluminum, a reduction of the Young's modulus is quite common when exposed to tensile stress.[58] The Young's modulus of oxides has also been found to change due to oxygen vacancies. In one study, the effect of oxygen vacancy to Young's modulus on CeO_2 was found to decrease the modulus from 264 GPa to 190 GPa.[59] The

Figure 6. Adhesion histograms. Blue bars represent adhesion measurements taken out of the defect region and red bars indicate adhesion within the defect region. a) pH 3. b) pH 5. c) pH 7. d) pH 10

increase of adhesion on alumina may be due to a similar phenomenon, in this case the hydroxides are inserting into the surface as bonds are impacted from the AFM tip.

In a similar study on mica, the adhesion in wear areas was also seen to increase. The authors attributed the change to two different factors. First, in regions of gross wear the alumina layer was exposed and would change the tip substrate interaction due to the different chemical environment. Second, none uniformity of defects would also create different chemical environments, which also was attributed to the greater spread of adhesion values.[60] Alumina is likely affected by none uniform defects on the surface, which would create a wider range of tip interactions with the surface. The chemical environment may also change significantly as the surface roughness increases. A possible explanation for the change in adhesion is that the surface roughness may develop quasi alumina particle properties. In a study comparing the IEP of single crystal alumina and alumina particles, the IEP of alumina particles was found to be around pH 9 and that of single crystal alumina to be at ~pH 5.[61] So, if the isoelectric point of the local surface changes, then a dramatic increase in the coulombic attraction may cause greater adhesion.

2.4 Summary

By incorporating the AFM, the influence of water on the tribological properties of wear and adhesion on the alumina (0001) surface was investigated. The results show that as the concentration of OH^- increases, the degradation of the alumina surface also increases, demonstrating the catalytic strength of OH^-. The pressure required to create 2

Å of wear on the surface decreased by ~1.5 GPa. The friction did not appear to change significantly in the defect region. Overall the adhesion measured on the polished alumina surface by the AFM probe was very small with a maximum adhesion occurring at pH 5 with an average adhesion of 1 nN. This is due to the small contact area occasioned by the 20-30 nm tips, large elastic moduli of alumina and silicon nitride, and is further affected by a very smooth alumina surface used in the study. The forces of adhesion approximately doubled in the defect zones independent of pH. The actual causes of the increase in adhesion are unknown due to presently unknown variables that act on the surface. Defects caused by the interaction of other surfaces with alumina will lead to increased adhesion, and as repetitive contact with alumina takes place increased wear will occur.

3. ANALYSIS OF PROTECTED ALUMINA SURFACE

3.1 Overview

The reaction of water with the oxidized surface of Al is a key pathway for the eventual degradation and corrosion of Al. One approach frequently employed in creating water resistant/repellent surfaces on oxides is to coat the surface with a long alkylsilane chain such as octadecyltrichlorosilane (OTS). Another approach is to utilize alkyl phosphonates to create water repellant surfaces, as the reactions of phosphonates with oxides are well known and provide a generally reliable means of attaching compounds to surfaces.

To evaluate the protective capabilities of these two materials SAMs of OTS and octadecylphosphonic acid (OPA) were created on Al_2O_3 (0001) surfaces and examined their surface composition, film morphology and stability using a combination of Fourier transform infrared spectroscopy (IR) and atomic force microscopy (AFM). The stability of the films were compared under aqueous environments with pH ranging from ~ 3 - 10. The pH 10 conditions mimic highly corrosive environments, as under these conditions, reactions between OH⁻ and the Si-O-Al or P-O-Al bonds formed between the monolayers and the surface are highly susceptible to the presence OH⁻, as hydroxide is known to catalyze metal-oxygen bond breaking.[7, 15, 62]

FTIR and AFM were employed to establish the stability of the SAMs under different environments. FTIR spectroscopic measurements of monolayers can be accomplished by the transmission of IR light through the sample, or by reflection from

the surface. Also, for alkyl based materials, the extent of film disorder can be deduced by measurement of the methylene (CH_2) symmetric and asymmetric stretch frequencies. For densely packed layers, the asymmetric stretch should emerge around 2918 cm^{-1} and will shift to higher wavenumbers with increasing disorder.[54]
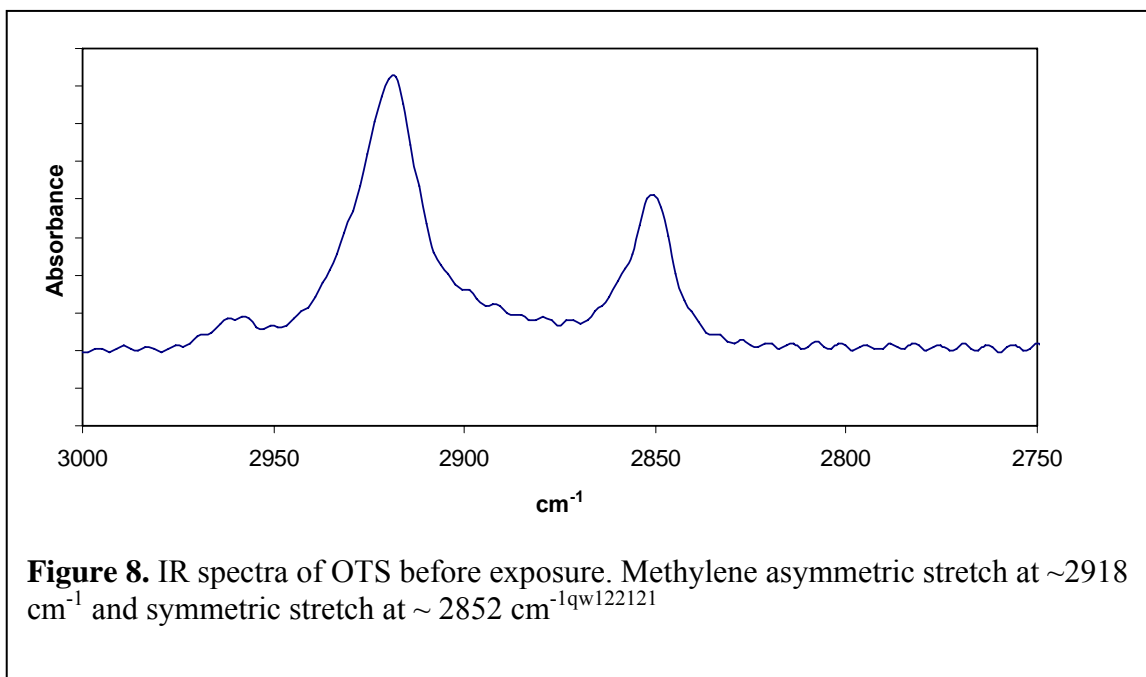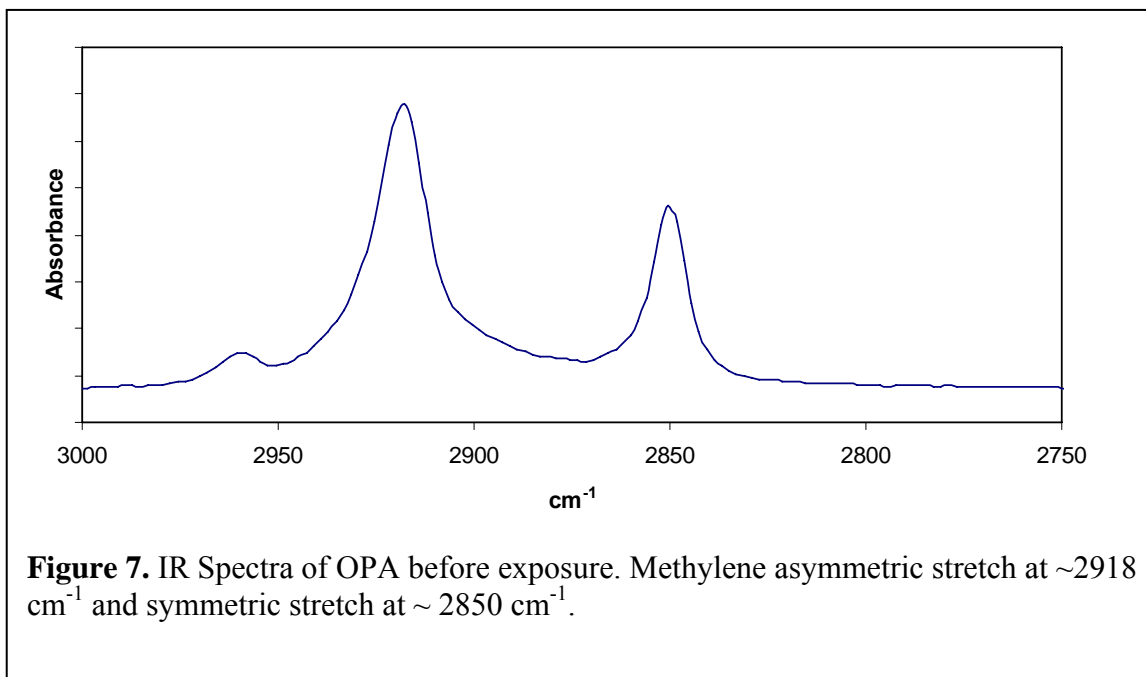
AFM measurements allow for the 3-D topography of samples to be directly obtained. In AFM, a sharp tip made of Si_3N_4 with a radius of curvature of approximately 25 nm is attached to a cantilever and is rastered over a surface by a piezoelectric scanner. The forces acting between the tip and surface are monitored by the deflection of a laser from the back of the cantilever-tip assembly and plotted as a function of the tip position to produce a topographic image. In addition to topography, the AFM tip can also be pressed against the surface to very high pressures (> 4 GPa) to induce wear of the surface. In this fashion the structural integrity of a material as well as its local hardness can be deduced.

In this study, rapid ageing of the films was examined by pressure induced wear by the AFM tip against the film surface to establish the relative stability of each for a given environment. IR measurements were conducted to first examine the organization of the SAM on the alumina surface and to then follow subsequent changes in the SAM on the surface after exposure to different environments. These measurements can also provide a means of determining if water is adsorbed on the surface of alumina.

3.2 Experimental

The sample preparation method was as follows: polished single crystal alumina (0001) substrates (Crystal Systems, Inc) were cleaned of all carbon contaminants. This cleaning process included 20min UV/ozone cleaning and 20min in a 4:1:1 solution of H_2O, H_2O_2 and NH_4OH at 85°C. The substrate was then rinsed with ultrapure water (18 MΩ*cm) and blown dry with nitrogen gas. Then the substrates were submerged in hexane solution and sonicated. As the solution was sonicated, 40 μL of OTS or OPA were added and the solution was sonicated for 3 hrs. After 3 hrs the substrates were placed in a THF bath and sonicated for an additional 30 min to clean the surface of physically absorbed molecules.

FTIR measurements were taken in a ThermoElectric *Nicolet 6700 FT-IR* in absorption mode. The alumina substrates were positioned at 60°, approximately the Brewster angle[63], so as to reduce the fringing that occurred by varying angles and to decrease reflection. The fresh SAM, OTS or OPA, was used as the background compare changes in the monolayer caused by the aqueous environments. Testing for the effect of aqueous environments on the stability of each respective SAM involved submersion of the substrate in an aqueous bath of defined pH for 30 min. The substrates were then analyzed by FTIR spectroscopy for the effect of the environment on the integrity of the monolayer and by AFM to image the surface. AFM images were taken in ambient environments before and after submersion in the aqueous bath and wear measurements were taken in aqueous conditions for OTS SAMs.

Figure 7. IR Spectra of OPA before exposure. Methylene asymmetric stretch at ~2918 cm^{-1} and symmetric stretch at ~ 2850 cm^{-1}.

Figure 8. IR spectra of OTS before exposure. Methylene asymmetric stretch at ~2918 cm^{-1} and symmetric stretch at ~ 2852 cm$^{-1qw122121}$
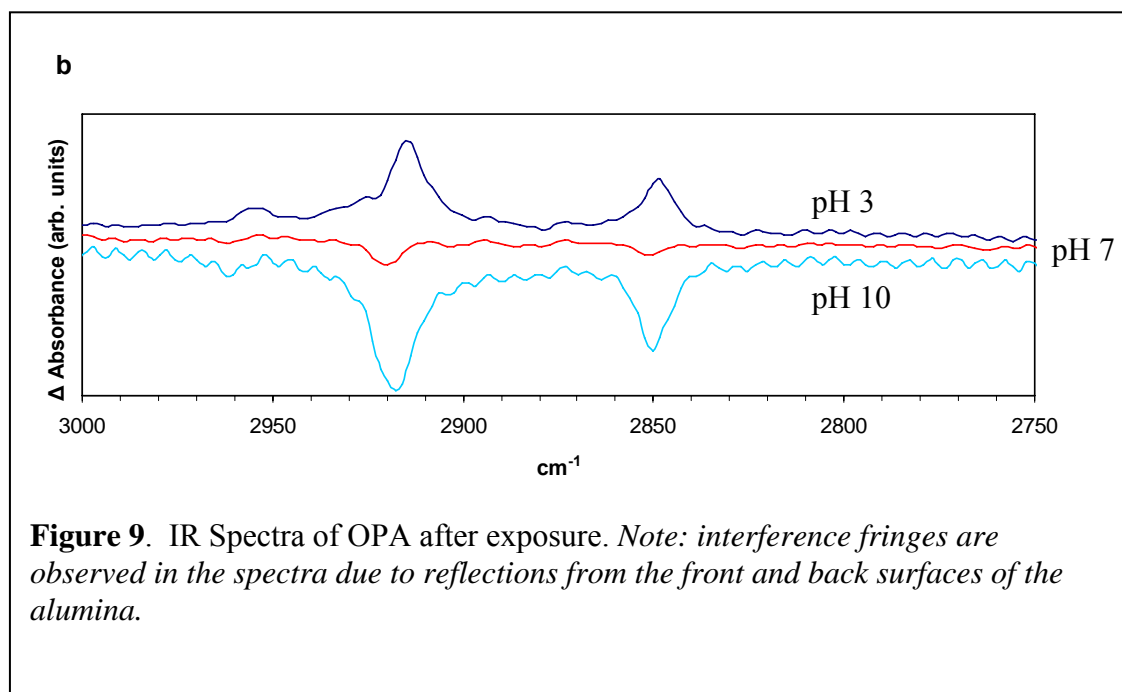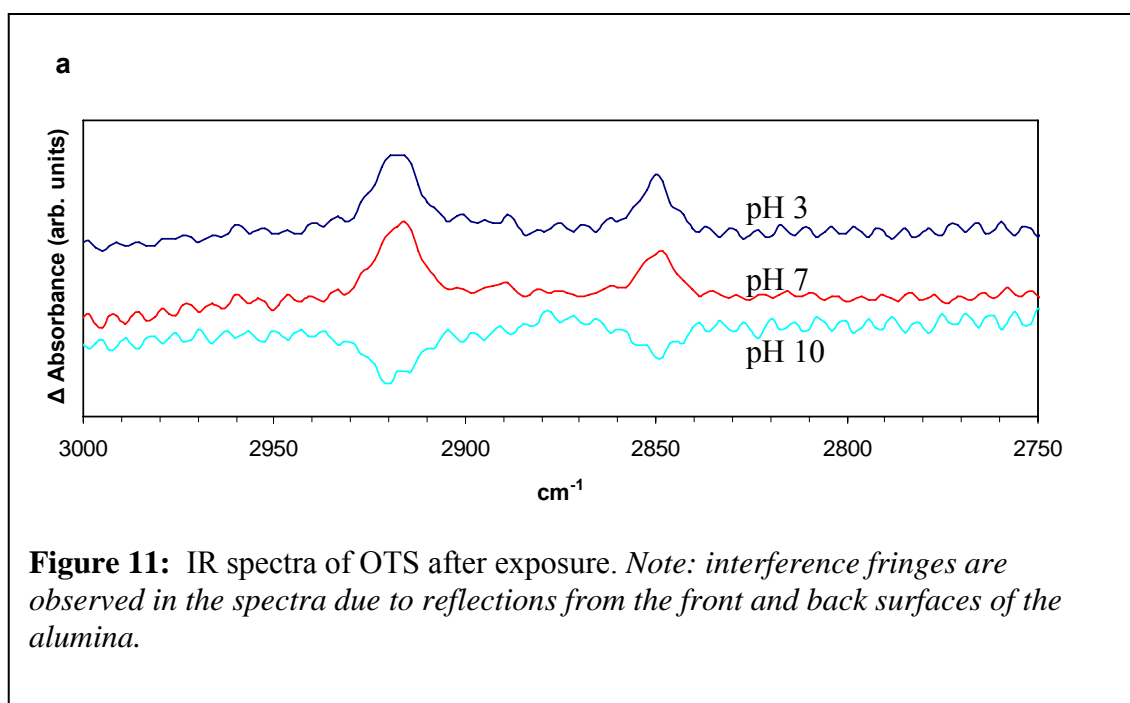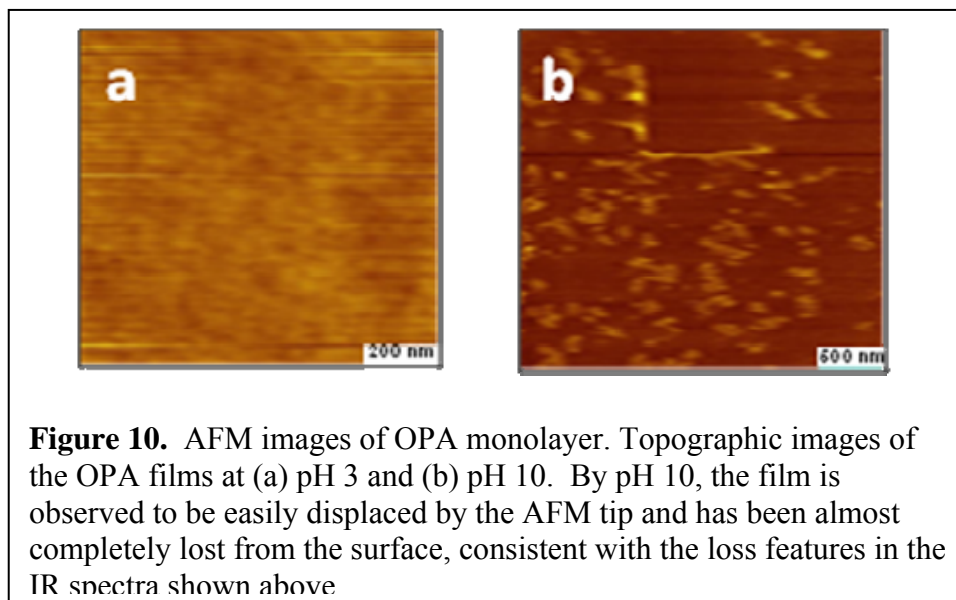
3.3 Results

IR measurements of the OPA and OTS films were taken before any exposure to aqueous environments as seen in Figures 7 and 8. The asymmetric stretches in both spectra are around 2919 cm^{-1}, which is the ideal location for a densely packed SAM. This indicates that the film on the surface is well ordered and should lead to a good approximation of each SAM's ability to protect the surface from wear and corrosion caused by exposure to aqueous environments.

IR measurements of the OPA films, post exposure, quickly ruled out the possibility of using OPA as a structurally sound anti-corrosion covering for surfaces that may be exposed to a caustic alkaline environment. Figure 9 shows a representative series of IR spectra for an OPA self-assembled monolayer after having been submerged for 1 hr in solutions with increasing pH, up to an NH_4OH solution at pH 10. The film was found to be stable both in air as well as under aqueous environments at pH 3. With increasing pH, the loss of the OPA from the surface was detected as the IR signals became negative relative to the initial film. The negative peaks for the CH_2 stretches at ca. 2850 cm^{-1} and 2918 cm^{-1} indicate the loss of OPA from the surface after exposure to elevated pH conditions. AFM images taken immediately after the IR spectra further support this conclusion. In Figure 10, AFM images taken on the OPA surface after exposure to aqueous environments is shown. At low pH the surface film was retained and shows a densely packed monolayer. By pH 10 however, little OPA was observed to remain on the surface as the IR signals are negative and the remaining film appears as

small islands which are easily displaced by the AFM tip indicating that they are weakly

bound to the surface.

Figure 9. IR Spectra of OPA after exposure. *Note: interference fringes are observed in the spectra due to reflections from the front and back surfaces of the alumina.*

Films of OTS on the alumina surface were found to be much more robust under

aqueous environments. As shown in Figure 11, no loss of the film was observed until

beyond pH 7. To evaluate the overall film stability, more in-depth AFM measurements

of the OTS SAM stability and resistance to wear were explored under the varying pH

environments. Here we explored OTS samples under four different pH environments (3,

7, 8, and 10). In order to rapidly age the films, increased loads were applied by AFM

Figure 10. AFM images of OPA monolayer. Topographic images of the OPA films at (a) pH 3 and (b) pH 10. By pH 10, the film is observed to be easily displaced by the AFM tip and has been almost completely lost from the surface, consistent with the loss features in the IR spectra shown above.

Figure 11: IR spectra of OTS after exposure. *Note: interference fringes are observed in the spectra due to reflections from the front and back surfaces of the alumina.*

over various test regions of the surface. Different loads up to approximately 10 nN (i.e.

local pressures on the films approximately 1 GPa) were applied to the film over a 400

nm x 400 nm test area on the surface for 10 cycles at a rate of 33 Hz. After each test, the

load was then reduced and a larger area, ca. 1 μm x 1 μm, was imaged to examine if the

film was damaged in any way. We compared these test under both ambient conditions

in air and in aqueous environments at the pH indicated above. For a baseline test, the

clean alumina surface was examined at pH 3 and pH 8, shown in Figure 12. As the

solution becomes more basic the surface is observed to readily wear under the pressures

applied by the AFM tip. As is observed in Figure 12d, an etch pit of only ca. 0.4 nm is

formed.

Figure 12. Baseline test of alumina. Topographical images taken a) Before image at pH 3. b) After scanning at 10nN at pH 3. c) Before image at pH 8. d) After scanning at 10nN at pH 8. e) Line trace of image d.
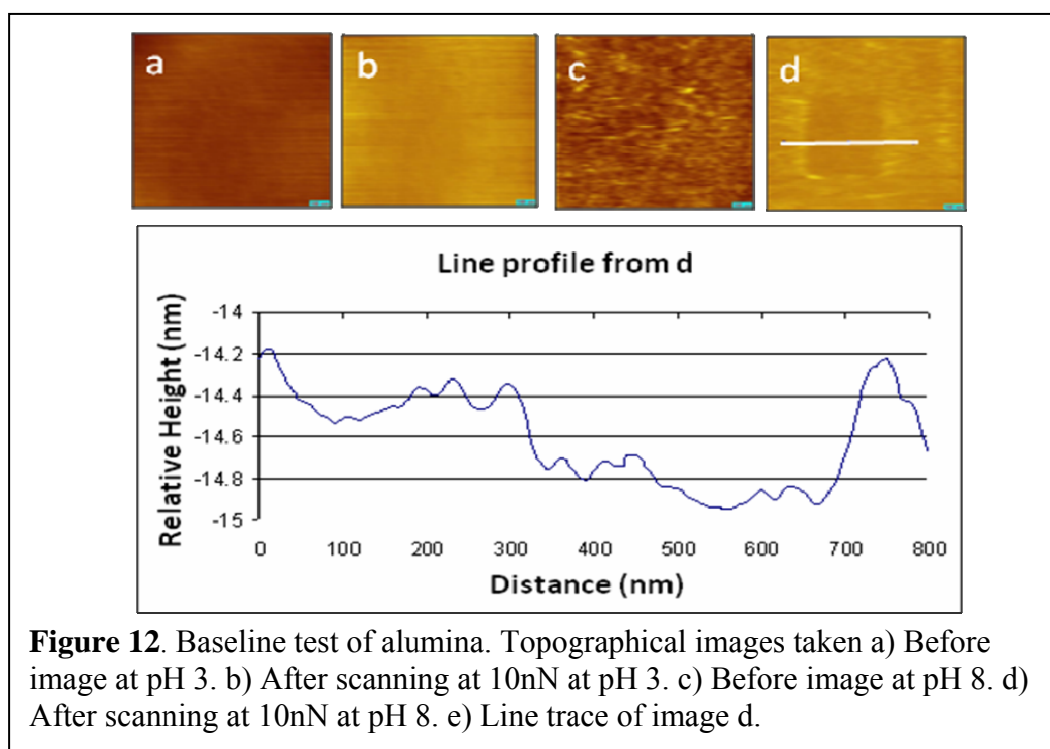
After applying the OTS SAM to the surface, some very encouraging results were obtained. Even though the IR measurements show some loss of OTS at pH 10, unlike the OPA films, the OTS SAMs remains reasonably intact on the surface, although it is now more disordered due to loss of materials. Figure 13 shows that after applying high pressures to the film, a hole in the test region was formed. The line trace indicates a film thickness of ca. 2 nm, consistent with the molecular chain length of the SAM. Thus
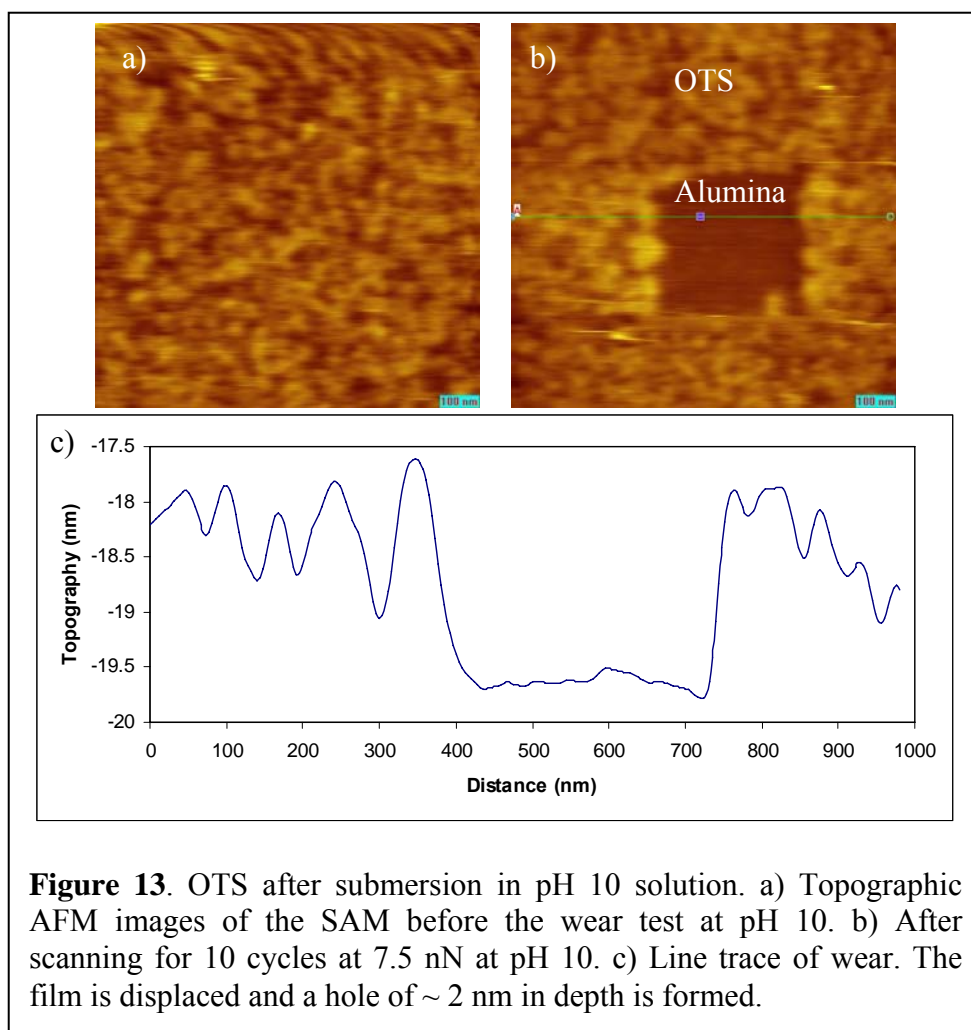

Figure 13. OTS after submersion in pH 10 solution. a) Topographic AFM images of the SAM before the wear test at pH 10. b) After scanning for 10 cycles at 7.5 nN at pH 10. c) Line trace of wear. The film is displaced and a hole of ~ 2 nm in depth is formed.

even under caustic environments, the OTS film can still resist complete loss from the surface, and is only displaced under high loads.

3.4 Summary

Films of OPA and OTS have been examined on alumina surfaces. OPA films were found to be unsuitable as protective layers under caustic environments. OTS films however were found to only partially degrade under high pH conditions and can provide a reasonable surface coating with little degradation until very high pH. The short chain length of the OTS ($\sim$ 2 nm) and high packing density on the surface ($\sim$ 3 molecules/nm^2) provide a means of increasing surface hydrophobicity and decreasing water film penetration. As such, these represent a viable means of forming a protective coating on the surface. While these measurements were made on single crystal alumina, they suggest that further investigation of their properties on more realistic oxidized Al surfaces are warranted, especially considering the relative ease of film formation and the low cost of preparing such coatings in piping. As compared to the monolayers on alumina (0001), the viability of OTS as a protective coating on Al loop-heat pipe surfaces however may be reduced considering the significant surface roughness of the pipes, as surface roughness reduces film order, which leads to increased numbers of film defects. One way to ameliorate this however may be to introduce chain branching on the silane to fill in the gaps formed when lower packing density films are created. The introduction of chain branching will also increase overall film durability through increased interchain hydrophobic interactions.

4. CONCLUSIONS

The regulation of environment is incredibly important for the future use of alumina in advancing technologies. The surface of alumina is dramatically affected by the environment to which it is exposed. In alkaline environments the surface is greatly affected by corrosion and wear as the OH^- molecules catalyze the rupture of Al-O bonds facilitating wear and degradation of the alumina surface. This is expressed in the decreased force required to create defects at approximately 1 GPa in a pH 10 environment. Through force distance spectroscopy, it was found that at pH 5 the adhesion was greatest with a work of adhesion of ~8 mN/m. In defect regions, adhesion approximately doubled at all pH environments tested. More research is needed to understand better the forces causing greater adhesion.

For protecting monolayers phosphonic acids are not an ideal candidate as they are rapidly displaced by competing hydroxide molecules. Except at low pH environments, where hydroxides are minimal, are SAMs of phosphonic acids remotely feasible. Silanes, on the other hand, were found to be very robust even in highly alkaline solutions. The application of silane monolayers is a simple, robust method to protect the alumina surface from the caustic effects of aqueous environments.

REFERENCES

(1)   Li, J. *MRS Bulletin* **2007,** *32* (2), 151-159.

(2)   Wang, A.; McAllister, J. P.; Finlayson, P.; Li, J.; Brabant, K.; Tang, H.; Black, C.; Cao, T.; Liang, X.; Salley, S. O.; Auner, G. W.; Ng, K. Y. S. *Materials Science & Engineering, C: Biomimetic and Supramolecular Systems* **2007,** *27* (2), 237-243.

(3)   Navarro, L. M.; Recio, P.; Jurado, J. R.; Duran, P. *J. Mater. Sci.* **1995,** *30* (8), 1949-60.

(4)   Franks, G. V.; Gan, Y. *J. Am. Ceram. Soc.* **2007,** *90* (11), 3373-3388.

(5)   Ni, C. H.; Chen, J. N. *Water Sci Technol FIELD Full Journal Title:Water Science and Technology : A Journal of the International Association on Water Pollution Research* **2001,** *43* (2), 213-20.

(6)   Gonzalez-Juarez, J. C.; Jimenez-Becerril, J.; Carrasco-Abrego, H. *J. Radioanal. Nucl. Chem.* **2008,** *275* (2), 257-260.

(7)   Kasprzyk-Hordern, B. *Adv. Colloid Interface Sci.* **2004,** *110* (1,2), 19-48.

(8)   Franks, G. V.; Meagher, L. *Colloids and Surfaces, A: Physicochemical and Engineering Aspects* **2003,** *214* (1-3), 99-110.

(9)   Veeramasuneni, S.; Yalamanchili, M. R.; Miller, J. D. *J. Colloid Interface Sci.* **1996,** *184* (2), 594-600.

(10)   Stack, A. G.; Higgins, S. R.; Eggleston, C. M. *Geochim. Cosmochim. Acta* **2001,** *65* (18), 3055-3063.

(11)   Stack, A. G.; Higgins, S. R.; Eggleston, C. M. *Geochim. Cosmochim. Acta* **2003,** *67* (2), 321-322.

(12)   Tulpar, A.; Henderson, D. B.; Mao, M.; Caba, B.; Davis, R. M.; Van Cott, K. E.; Ducker, W. A. *Langmuir* **2005,** *21* (4), 1497-1506.

(13)   Kershner, R. J.; Bullard, J. W.; Cima, M. J. *Langmuir* **2004,** *20* (10), 4101-4108.

(14)   Yeganeh, M. S.; Dougal, S. M.; Pink, H. S. *Phys. Rev. Lett.* **1999,** *83* (6), 1179-1182.

(15)   Fischer, T. E.; Mullins, W. M. *J. Phys. Chem.* **1992,** *96* (14), 5690-701.

(16)   Madsen, L.; Blokhus, A. M. *J. Colloid Interface Sci.* **1994,** *166* (1), 259-62.

(17) Hintze, P. E.; Calle, L. M. *Electrochim. Acta* **2006,** *51* (8-9), 1761-1766.

(18) Chen, H.; Wang, J.; Huo, Q. *Thin Solid Films* **2007,** *515* (18), 7181-7189.

(19) Vaidya, R. U.; Brozik, S. M.; Deshpande, A.; Hersman, L. E. *Corrosion (Houston, TX, United States)* **2001,** *57* (10), 905-912.

(20) Hoque, E.; DeRose, J. A.; Kulik, G.; Hoffmann, P.; Mathieu, H. J.; Bhushan, B. *Journal of Physical Chemistry B* **2006,** *110* (22), 10855-10861.

(21) Cooper, R. J.; Camp, P. J.; Henderson, D. K.; Lovatt, P. A.; Nation, D. A.; Richards, S.; Tasker, P. A. *Dalton Transactions* **2007,** (13), 1300-1308.

(22) Pellerite, M. J.; Dunbar, T. D.; Boardman, L. D.; Wood, E. J. *Journal of Physical Chemistry B* **2003,** *107* (42), 11726-11736.

(23) Luschtinetz, R.; Seifert, G.; Jaehne, E.; Adler, H.-J. P. *Macromolecular Symposia* **2007,** *254* (Reactive Polymers in Inhomogeneous Systems in Melts, and at Interfaces), 248-253.

(24) Sun, S.; Leggett, G. J. *Nano Letters* **2007,** *7* (12), 3753-3758.

(25) Brukman, M. J.; Marco, G. O.; Dunbar, T. D.; Boardman, L. D.; Carpick, R. W. *Langmuir* **2006,** *22* (9), 3988-3998.

(26) Felhosi, I.; Keresztes, Z.; Kalman, E. *Proc. - Electrochem. Soc.* **2001,** *2001-22* (Corrosion and Corrosion Protection), 386-392.

(27) Luschtinetz, R.; Oliveira, A. F.; Frenzel, J.; Joswig, J.-O.; Seifert, G.; Duarte, H. A. *Surf. Sci.* **2008,** *602* (7), 1347-1359.

(28) Foster, T. T. Structure and Stability of Self-Assembled Monolayers on Gold, Silver and Aluminium Oxide Surfaces. University of Manchester Institute of Science and Technology, 2004.

(29) Minor, A. M. A., S. A. Syed; Shan, Zhiwei; Stach, Eric A.; Cyrankowski, Edward; Wyrobek; Thomas J and Warren, O. L. *Nature Materials* **2006,** *5*, 697-702.

(30) Ogata, S.; Li, J.; Hirosaki, N.; Shibutani, Y.; Yip, S. *Physical Review B: Condensed Matter and Materials Physics* **2004,** *70* (10), 104104/1-104104/7.

(31) Rice, R. *J. Am. Ceram. Soc.* **1991,** *77* (10), 2539-2553.

(32) Eiss, N. S., Jr.; Fabiniak, R. C. *J. Am. Ceram. Soc.* **1966,** *49* (4), 221-6.

(33)   Voloshin, A. V.; Lytvynov, L. A. *Functional Materials* **2002,** *9* (3), 554-555.

(34)   Zhoua, Y.; Atwood, M.; Golini, D.; Smith, M.; Funkenbusch, P. D. *Wear* **1998,** *219* (1), 42-45.

(35)   Carpick, R. W.; Dai, Q.; Ogletree, D. F.; Salmeron, M. *Tribology Letters* **1998,** *5* (1), 91-102.

(36)   Carpick, R. W.; Enachescu, M.; Ogletree, D. F.; Salmeron, M. *Materials Research Society Symposium Proceedings* **1999,** *539* (Fracture and Ductile vs. Brittle Behavior--Theory, Modelling and Experiment), 93-103.

(37)   Carpick, R. W.; Salmeron, M. *Chemical Reviews (Washington, D. C.)* **1997,** *97* (4), 1163-1194.

(38)   DeVecchio, D.; Bhushan, B. *Rev. Sci. Instrum.* **1998,** *69* (10), 3618-3624.

(39)   Erlandsson, R.; Hadziioannou, G.; Mate, C. M.; McClelland, G. M.; Chiang, S. *J. Chem. Phys.* **1988,** *89* (8), 5190-3.

(40)   Gao, G.; Cannara, R. J.; Carpick, R. W.; Harrison, J. A. *Langmuir* **2007,** *23* (10), 5394-5405.

(41)   Helt, J. M.; Batteas, J. D. *Langmuir* **2005,** *21* (2), 633-639.

(42)   Hu, J.; Xiao, X. d.; Ogletree, D. F.; Salmeron, M. *Surf. Sci.* **1995,** *327* (3), 358-70.

(43)   Miyake, S. *Appl. Phys. Lett.* **1994,** *65* (8), 980-2.

(44)   Park, N.-S.; Kim, M.-W.; Langford, S. C.; Dickinson, J. T. *J. Appl. Phys.* **1996,** *80* (5), 2680-2686.

(45)   Park, N.-S.; Kim, M.-W.; Langford, S. C.; Dickinson, J. T. *Langmuir* **1996,** *12* (19), 4599-4604.

(46)   Prioli, R.; Reigada, D. C.; Freire, F. L., Jr. *Appl. Phys. Lett.* **1999,** *75* (9), 1317-1319.

(47)   Carpick, R. W.; graiet, N.; Ogletree, D. F.; Salmeron, M. *Journal of Vacuum Science & Technology, B: Microelectronics and Nanometer Structures* **1996,** *14* (2), 1289-1295.

(48)   Dickinson, J. T.; Hariadi, R. F.; Langford, S. C. *Ceram. Trans.* **1999,** *102* (Finishing of Advanced Ceramics and Glasses), 213-232.

(49) Marti, A.; Haehner, G.; Spencer, N. D. *Langmuir* **1995,** *11* (12), 4632-5.

(50) Maw, W.; Stevens, F.; Langford, S. C.; Dickinson, J. T. *J. Appl. Phys.* **2002,** *92* (9), 5103-5109.

(51) Johnson, K. L. *Proceedings - Institution of Mechanical Engineers* **1982,** *196*, 363-378.

(52) Johnson, K. L.; Kendall, K.; Roberts, A. D. *Proceedings of the Royal Society of London, Series A: Mathematical, Physical and Engineering Sciences* **1971,** *324* (1558), 301-13.

(53) Derjaguin, B. V. M., V. M.; Toporov, YU. P. *J. Colloid Interface Sci.* **1975,** *53* (2), 314-326.

(54) Nuzzo, R. G.; Dubois, L. H.; Allara, D. L. *J. Am. Chem. Soc.* **1990,** *112* (2), 558-69.

(55) Hertz, H. *J. Rein Angew. Math.* **1881,** *92*, 156.

(56) Johnson, K. L., *Contact Mechanics*. Cambridge University Press: Cambridge, 1987.

(57) Sheiko, S. S.; Moeller, M.; Reuvekamp, E. M. C. M.; Zandbergen, H. W. *Physical Review B: Condensed Matter and Materials Physics* **1993,** *48* (8), 5675-8.

(58) Benito, J. A.; Manero, J. M.; Jorba, J.; Roca, A. *Metallurgical and Materials Transactions A: Physical Metallurgy and Materials Science* **2005,** *36A* (12), 3317-3324.

(59) Wang, Y.; Duncan, K.; Wachsman, E. D.; Ebrahimi, F. *Solid State Ionics* **2007,** *178* (1-2), 53-58.

(60) Helt, J. M. a. B., James D. *Langmuir* **2006,** *22*, 6130-6141.

(61) Franks, G. V. a. M., Laurence. *Colloids and Surfaces A* **2003,** *214*, 99-110.

(62) Hass, K. C. S., W. F.; Curioni, Alessandro; Andreoni, Wanda. *Science (Washington, DC, United States)* **1991,** *282*, 265-268.

(63) Patel, B. S.; Zaidi, Z. H. *Measurement Science and Technology* **1999,** *10* (3), 146-151.

VITA

Name: Ammon Terry Pickett

Address: Clear Lake High School
                         2929 Bay Area Blvd.
                         Houston, TX 77058

Email Address: ammonpickett@hotmail.com

Education: B.S., Chemistry, Southern Utah University, Cedar City, 2005
                         M.S., Chemistry, Texas A&M University, College Station, 2008